

Eq. (6).

$$f(X, \Delta) = \frac{1}{2\pi i} \int_{-i\alpha+\delta}^{+i\alpha+\delta} \times \exp \left\{ p\Delta - x \int_0^\alpha \omega(\epsilon) [1 - \exp(-p\epsilon)] d\epsilon \right\} dp. \quad (6)$$

For a substance that consists of a mixture of several constituents, we say that

$$\omega(\epsilon) = \sum \omega_i(\epsilon) = \sum_i \frac{2\pi N e^4 \rho_i \sum Z_i}{m v^2 \sum A_i \epsilon^2}, \quad (7)$$

where the summation over  $i$  refers to the sum over  $i$  constituents.

Making use of Eq. (7) in (6), we find that the function has its maximum at

$$\Delta = \Delta_0 = \sum_i \frac{\eta_i}{\beta^2} \left[ \ln \frac{5.5 \times 10^6 \eta}{I_i^2 (1 - \beta^2)} + 1 - \beta^2 \right], \quad (8)$$

where the symbols are those defined in Eq. (1).

#### Density Effect

In order to calculate the density-effect corrections to the most probable loss, we turn to the Sternheimer treatment.<sup>5</sup> In this paper the reduction in energy loss due to the polarization of the medium is described as

$$\Delta \left( \frac{dE}{dx} \right) = \frac{2\pi n e^4}{m v^2} \left[ \sum_i f_j \left( \frac{\bar{\nu}_j^2 + l^2}{\bar{\nu}_j^2} \right) - l^2 (1 - \beta^2) \right], \quad (9)$$

where  $n$  is the number of electrons per  $\text{cm}^3$ ,  $m$  is the electron mass,  $f_j$  is the oscillator strength of the  $j$ th transition, whose frequency is  $\nu_j$ , and  $l$  is a frequency that is the solution of the equation

$$\frac{1}{\beta^2} - 1 = \sum_i \frac{f_j}{\nu_j^2 + l^2}. \quad (10)$$

Here  $\nu_j$  is to be expressed in terms of the plasma frequency of the medium, ( $\bar{\nu}_j = \nu_j / \nu_p$ ),

$$\nu_p = (n e^2 / \pi m)^{1/2}. \quad (11)$$

We wish to calculate the density effect of our particular counter filling, a mixture of helium and carbon dioxide. Since the density effect is largely the result of the so-called distant collisions, we propose to treat the gas filling as a homogeneous mixture of  $\text{CO}_2$  and helium and not distinguish between a  $\text{CO}_2$  collision and a helium collision. This reduction in energy loss for the mixture is then subtracted from Eq. (8) for the most probable total loss. This is done by defining

$$\delta_{\text{mix}} = \sum_j f_j \ln \left[ \frac{\bar{\nu}_j^2 + l^2}{\bar{\nu}_j^2} - l^2 (1 - \beta^2) \right]; \quad (12)$$

the net result is then Eq. (1). Note that  $\eta \delta_{\text{mix}}$  differs from  $\sum_i \eta_i \delta_i$  in that the plasma frequency is that of the total mixture and therefore  $\bar{\nu}_j$  of Eq. (12) are different from those for the constituents alone. For the counter filling used in this experiment, the difference is negligible.

### Capture and Decay of $\mu^-$ Mesons in Fe $\dagger$

W. A. BARRETT,\* F. E. HOLMSTROM, AND J. W. KEUFFEL  
 University of Utah, Salt Lake City, Utah

(Received September 2, 1958)

The mean life of  $\mu^-$  mesons in Fe has been measured using an improved cosmic-ray apparatus. A positive identification of the stopped muon was made using Čerenkov velocity selectors in the incident telescope. The 2.2- $\mu\text{sec}$  background from positive muons was reduced a factor of 3 with a 3-layer sandwich of Fe and thin plastic scintillators, so arranged that electrons emitted in the target were mostly detected as such by the scintillators. The mean life is  $196 \pm 8 \mu\text{sec}$ . By comparing this result with the electron-counting results of Lederman and Weinrich, the ratio of the decay rate of  $\mu^-$  bound in Fe to the free  $\mu^-$ -decay rate is found to be  $1.15 \pm 0.06$ .

#### I. INTRODUCTION

WHEN a negative muon comes to rest in condensed matter, it falls rapidly to the mesonic  $K$  orbit of an atom. From here it may undergo nuclear capture

or it may undergo spontaneous decay. The rate  $\lambda$  at which the mesons disappear is the sum of the capture rate,  $\lambda_c$ , and the rate  $\lambda_d$  for spontaneous decay;  $\lambda_d$  is usually taken as equal to the decay rate  $\lambda_0$  of the free positive muon in order that  $\lambda_c$  may be obtained from the measured values of  $\lambda$ . Only recently has attention been focused on  $\lambda_d$  and the extent to which it may deviate from  $\lambda_0$ .

$\dagger$  Assisted by the National Science Foundation.

\* University Research Committee Fellow. Now at Bell Telephone Laboratories, Murray Hill, New Jersey. This paper is based on a Ph.D. thesis submitted to the faculty of the University of Utah, (1957), by W. A. Barrett.

The value of  $\lambda_d$  for a given  $Z$  may be obtained by combining a measurement of the branching ratio for capture and decay with an accurate value of  $\lambda$ , since the fraction  $f_d$  of muons undergoing decay is just  $\lambda_d/\lambda$ . Values of  $f_d$  have been measured by Lederman and Weinrich<sup>1</sup> for a number of elements, including Fe. The purpose of the present work was to measure  $\lambda$  accurately for Fe, so that a value of  $\lambda_d$  might be obtained.

During the course of our work, measurements of  $\lambda$  were carried out by the Chicago group<sup>2</sup> for a number of elements, including Fe. These authors<sup>3</sup> also recently measured  $\lambda_d$  by a technique involving the simultaneous measurement of the numbers and delay distributions of the electrons from a "sandwich" target of light and heavy elements. Our results confirm the results of the Chicago group, both as to the value of  $\lambda$  for Fe and—when we combine  $\lambda$  with the Columbia  $f_d$  result—as to the value of  $\lambda_d$ .

The experimental results for Fe ( $Z=26$ ) are in disagreement with existing theoretical estimates<sup>4-6</sup> of  $\lambda_d$ . The theory predicts, for all  $Z$ , a *slower* decay for bound muons than for free ones, while for Fe (but not for heavier elements) an effect of the opposite sign is observed. The theory takes into account the reduction in accessible volume of phase space due to the binding, and the relativistic time dilation due to orbital motion of the muon. Telegdi's group has suggested that the Coulomb distortion of the wave function of the outgoing electron is responsible for the reverse effect, but quantitative calculations have not yet been made. In particular, it remains to be shown how  $\lambda_d$  can be 15–20% greater than  $\lambda_0$  for  $Z=26$  and less than  $\lambda_0$  for  $Z \geq 30$ , as appears to be the case experimentally.

The present experiment follows the basic technique of Keuffel *et al.*<sup>7</sup> (hereafter referred to as KHGR) in which the disappearance of the negative muon is signalled by a neutron or  $\gamma$  ray resulting from capture. The decay curve of the capture radiation gives the mean life, whose reciprocal is  $\lambda$ . This technique takes advantage of the low neutron backgrounds of cosmic-ray experiments. The workers at the machines use the decay electrons of those mesons which escape capture (a very small percentage in the case of medium and heavy elements) to follow the disappearance of the muons. Since these techniques are quite different, we deemed it worthwhile to report briefly at this time the result for a single element as a check on possible

systematic errors in the work done with the more copious machine mesons. It is interesting to note, however, that the Chicago group took about the same running time (three weeks) to measure 27 elements as was required (with comparable accuracy) in our single measurement. In view of the limitations on machine time the disparity in rates is not altogether discouraging. A larger cosmic-ray apparatus with several times the present rate has been constructed, and is now in operation.

In the present work, the original technique of KHGR has been improved in three important respects. First, the identification of the stopping muon has been made much more positive by the use of Čerenkov velocity selectors in the incident telescope. Second, the 2.2- $\mu$ sec background of delayed  $\gamma$  rays produced by bremsstrahlung following  $\mu^+$  decay has been reduced. And third, the delayed neutrons and  $\gamma$  rays used to signal the capture event have been separated from ionizing radiations by pulse-height selection, thus permitting the target and detector to be brought close together without the intervening anti-coincidence counter heretofore employed

## II. APPARATUS

The experiment was set up at the University of Utah (altitude 4700 ft). The counter disposition is shown in Fig. 1. The method of measurement employed is to note the time of arrival of a muon stopping in the target, as signalled by a pulse from the scintillation counter  $S_1$ , and then to record the time elapsed to the detection of an evaporation neutron (or  $\gamma$  ray) from  $\mu^-$  capture in the target. The neutron is detected by  $S_4$ , a liquid scintillator.

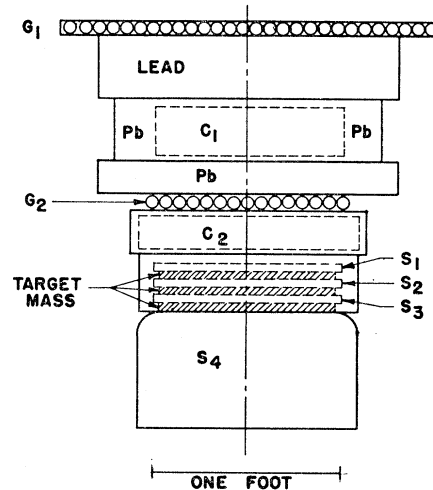


FIG. 1. Counter disposition. The Geiger counter trays  $G_1$  and  $G_2$ , the Čerenkov counters  $C_1$  and  $C_2$ , and the scintillators  $S_1$ ,  $S_2$  and  $S_3$  are square. Counter  $S_4$  is circular in cross section. A muon about to stop in the target gives a count in  $G_1$ ,  $C_1$ ,  $G_2$ , and  $S_1$ , but not in  $C_2$ . The capture radiation is detected in  $S_4$ . A  $\mu^+$  decay in the target will usually be recognized by a delayed count in  $S_2$ ,  $S_3$ , or a large pulse in  $S_4$ .

<sup>1</sup> L. M. Lederman and M. Weinrich, *Proceedings of the CERN Symposium on High-Energy Accelerators and Pion Physics, Geneva, 1956* (European Organization of Nuclear Research, Geneva, 1956), Vol. 2, p. 427.

<sup>2</sup> Sens, Swanson, Telegdi, and Yovanovitch, *Phys. Rev.* **107**, 1464 (1957).

<sup>3</sup> Lundy, Sens, Swanson, Telegdi, and Yovanovitch, *Phys. Rev. Lett.* **1**, 102 (1958).

<sup>4</sup> C. E. Porter and H. Primakoff, *Phys. Rev.* **83**, 849 (1951).

<sup>5</sup> Muto, Tanifuji, Inoue, and Inoue, *Progr. Theoret. Phys. Japan* **8**, 13 (1952).

<sup>6</sup> N. D. Khuri and A. S. Wightman (private communication).

<sup>7</sup> Keuffel, Harrison, Godfrey, and Reynolds, *Phys. Rev.* **87**, 942 (1952).

A simplified block diagram of the electronics is shown in Fig. 2. An oscilloscope sweep is triggered by a coincidence  $G_1\bar{C}_1G_2\bar{C}_2S_1S_4$  (the bar denotes an anti-coincidence), and delay-line shaped pulses from  $S_1$ ,  $S_2$ ,  $S_3$ , and  $S_4$  are separately delayed and displayed. Delays in  $S_4$  relative to  $S_1$  are then measured on a 35-mm photograph of the cathode-ray tube trace. The  $S_4$  pulse in the above triggering requirement is required to fall within a certain pulse-height interval, but all time delays of  $S_4$ , from  $-1$  to  $+10 \mu\text{sec}$  (relative to  $S_1$ ) are displayed and photographed. To read delays greater than  $3 \mu\text{sec}$ , a marker pulse with a fixed time delay relative to  $S_1$  is displayed to establish the (virtual) trace position of  $S_1$ .

### A. Selection of a Pure $\mu$ -Meson Beam

The counters  $G_1$ ,  $G_2$ , and  $S_1$  together with the 4-in. Pb filter (Fig. 1) define a cosmic-ray beam consisting mainly of muons with a small admixture of protons and electrons. With the addition of the anticoincidence Čerenkov counter  $C_2$ , the beam is restricted to particles with velocities less than the Čerenkov threshold for water (the threshold for  $C_2$  was about  $0.87c$ ). Further strong discrimination against electrons is thus provided, particularly since a soft shower event must contain ionizing particles at  $G_2$ , not at  $C_2$ , and then again at  $S_1$  with no heavy converters between them. For muons, the  $C_2$  anticoincidence condition means that the vast majority of fast mesons are eliminated. Slow mesons about to stop in the target are accepted, even including a meson incident at a 45-degree angle which stops in the bottom of the target.

Some discrimination against slow protons is obtained by demanding a "yes" count from the Čerenkov counter  $C_1$ , located above  $C_2$  and separated from it by 3 inches of common firebrick. A proton with sufficient velocity to trigger  $C_1$  would be incapable of stopping in any of the target plates without suffering a nuclear interaction. Fortunately, there were very few proton events of any sort, and delayed events from this source proved to be negligible. A stopping proton produces unusually large  $S_1$ ,  $S_2$ , or  $S_3$  pulses, and thus can often be positively identified (see Sec. III).  $C_1$  also helps eliminate soft-component events since it is completely surrounded by Pb.

The present stringent requirements on the nature of the incident particle are a considerable improvement over the work of KHGR and other  $\mu$ -capture experiments which relied mainly on the detection of delayed nonionizing radiation to identify the event sought. There are other events which have associated with them neutrons in the Mev region. These constitute a serious background if the neutrons are produced a few feet away from the counters since the time of flight of a 1-Mev neutron is about  $20 \mu\text{sec ft}^{-1}$ . Meyer,<sup>8</sup> using a hodoscope and a lead plate "sandwich" above a

KHGR-type apparatus, found spurious time lags of  $100 \mu\text{sec}$  or more connected with small soft events. Presumably these were the fringes of larger electron-photon showers which generated neutrons by the "giant resonance" ( $\gamma, n$ ) reaction near the core.

Much light was shed on this and other neutron-producing mechanisms by the experiment of Althaus and Sard,<sup>9</sup> using a neutron-triggered cloud chamber at sea level. For every detected neutron associated with  $\mu$ -capture these authors found about 4 neutrons from proton-induced stars, 15 neutrons from "low-energy events" (mostly electronic component) and 20 neutrons from fairly energetic electron cascades in their multi-plate chamber. In our experiment, dense electron showers (Sard's "high-energy cascades") produce large pulses in  $S_4$  and so are rejected because they exceed the upper threshold of the  $S_4$  pulse-height window. However, we rely on the tight  $\mu$ -selection conditions of the incident telescope to discriminate against the other neutron-producing events.

Neutrons may also be produced by fast  $\mu$  mesons in the lead above our apparatus, but the Čerenkov anticoincidence counter is very effective in cutting out fast mesons, or indeed even soft component which is secondary to the fast meson. Furthermore, the time lags from this process, as with the other processes where the neutrons are *locally* produced, should be very short compared to the minimum time-lag accepted for analysis in the  $\mu$ -meson decay curve ( $90 \mu\text{sec}$ ). Only reasonably fast neutrons ( $E > 0.75 \text{ Mev}$ ) were accepted by  $S_4$ .

Note also that a neutron generated above  $C_1$  usually has two water barriers to penetrate ( $C_1$  and  $C_2$ ) as well as the hydrogenous counters  $S_1$ ,  $S_2$ , and  $S_3$  before reaching  $S_4$ .

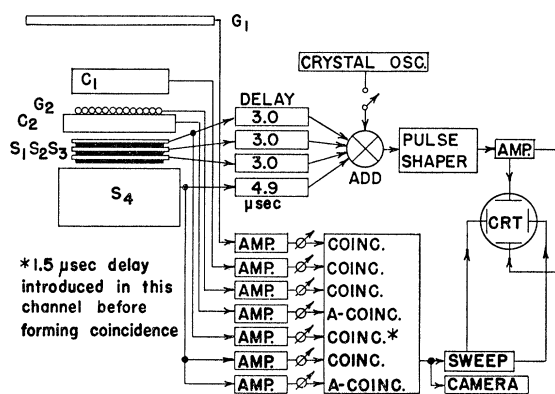


FIG. 2. Block diagram of the electronics. The coincidence circuit (lower portion of diagram) selects muons entering the incident telescope and stopping in the target. Pulses from the four scintillation counters are displayed on a fast oscilloscope sweep, permitting the determination of a mean life. Artificial delays separate the pulses and permit the sweep to get started before the pulses arrive. The delays actually used were 3.0, 3.6, 4.2, and  $4.9 \mu\text{sec}$  (not as shown).

<sup>8</sup> A. J. Meyer, thesis, Princeton University, 1954 (unpublished).

<sup>9</sup> E. J. Althaus and R. D. Sard, Phys. Rev. **91**, 373 (1953).

TABLE I. Counting rates for different types of events.

	Rate hr <sup>-1</sup>	Total rate hr <sup>-1</sup>
I. "Accepted" events (based on a 382-hr sample)		22.0
a. Time-zeros <sup>a</sup>	8.9	
b. 0.20- $\mu$ sec component ( $\mu^-$ capture)	6.7	
c. 2.22- $\mu$ sec component ( $\mu^+$ decay)	4.7	
d. Random noise (flat, from 0 to +10 $\mu$ sec)	1.7	
II. "Rejected" events (based on a 40-hr sample)		19.9
a. $S_1$ , $S_2$ , or $S_3$ delays	11.8	
b. $S_4$ pulse height too large	2.5	
c. No $S_4$ pulse or identified negative $S_4$ lags	2.4	
d. Double $S_4$	1.1	
e. $S_4$ only or blanked trace (misc.)	1.2	
f. $S_1$ or $S_2$ or $S_3$ pulse height too large (protons)	0.6	
g. $S_1$ and $S_3$ but no $S_2$ (soft component)	0.3	

<sup>a</sup> "Time-zeros" are the residual points near the origin after the extrapolated muon capture curve was subtracted from the data. The rates quoted for all events which have an exponential time distribution have been extrapolated to include counts with all delays from the origin to infinity. The observed rate of muon captures was 4.1 hr<sup>-1</sup>.

We shall see in Sec. III that contamination from any of the sources discussed above is indeed negligible.

### B. Rejection of Stopped $\mu^+$ Events

Rather than use a magnetic field to reject positive muons (which would reduce the  $\mu$ -acceptance solid angle drastically),  $\mu^+$  particles are rejected by detecting their decay positron in  $S_1$ ,  $S_2$ ,  $S_3$ , or  $S_4$ . The first three of these counters are thin plastic scintillators which are insensitive to neutrons from  $\mu$  capture. A pulse large enough to exceed the upper threshold of  $S_4$  can rarely be produced by a neutron. By dividing the target into thin layers, we reduce the chance that a bremsstrahlung  $\gamma$  ray should escape from the target without the detection of the decay positron that produced it. Such  $\gamma$  rays result in a background of 2.2- $\mu$ sec mean life.

The pulses from  $S_1$ ,  $S_2$ , and  $S_3$  are artificially delayed and displayed separately. An event exhibiting a shift in one or more of these pulses is rejected.

### C. Neutron Detector

The neutron detector  $S_4$  is a liquid scintillator with a sensitive volume 7 in. deep and 15 in. in diameter. It utilizes two 5-in. 6364 photomultipliers. The container<sup>10</sup> is made of iron 0.6 g/cm<sup>2</sup> thick coated with 0.12 g/cm<sup>2</sup> of porcelain enamel inside and out. An ionization loss of 100 kev results in about 20 photoelectrons.

The energy window in  $S_4$  extended from 0.15 to 1.1 Mev for electrons or, because of the nonlinearity of the scintillator, about 0.75 to 4 Mev for recoil protons. A study of the  $S_4$  pulse heights from capture events revealed that a higher upper threshold would result in few additional neutrons detected. The lower threshold appeared to give an optimum efficiency, in view of the scintillator nonlinearity of response to low-energy pro-

ton recoils and its sensitivity to low-energy soft background. The capture pulse-height spectrum was qualitatively an exponential, as one might expect of evaporation neutrons. However, nuclear  $\gamma$  rays (which also follow the  $\mu^-$ -decay curve) may have contributed an appreciable fraction of the total counts.

The energy window of  $S_4$  was such as to reject charged particles with high efficiency. For example, the pulse from a slow muon which penetrated  $S_4$  to a depth greater than 0.2 mm would exceed the upper threshold. It was therefore possible to dispense with the anti-coincidence Geiger counters between the target and  $S_4$  which were used in previous work<sup>7,8,11</sup> to establish the nonionizing nature of the delayed counts.  $S_4$  could then be placed close to the target, with a good solid angle and with no extraneous target materials present.

### D. Energy and Time Calibrations

Each of the scintillator and Čerenkov counters was calibrated by measuring the pulse-height distribution produced by normally-incident fast  $\mu$  mesons. The calibrations were checked daily by measuring an appropriate counting rate for each counter after the triggering thresholds had been checked with a mercury switch pulser.

The oscilloscope sweep was calibrated with a 2-Mc/sec ringing circuit, which was in turn compared with a crystal oscillator. A detailed study of the over-all time measurement procedure indicated that errors from this source should contribute no more than 0.25% to the error in the mean life. Several photographs of the ringing-circuit output were taken at the beginning of each day's run.

### III. RESULTS

In reading the film, events with a delayed pulse in  $S_1$ ,  $S_2$ , or  $S_3$  were rejected, along with a number of other less frequent types of events as indicated in Table I. The " $S_1$ ,  $S_2$ , or  $S_3$  delays" represented  $\mu^+$  decays in the Fe target, or  $\mu^\pm$  decays where the muons stopped in the scintillators themselves. Their time distribution followed a 2.2- $\mu$ sec exponential. From the table, it is seen that they are twice as numerous as the 2.2- $\mu$ sec component in the accepted events, so that the scintillator sandwich reduced the  $\mu^+$  bremsstrahlung background by a factor of 3.

Also rejected were events with  $S_4$  larger than 1.1-Mev (the upper threshold in the triggering system was slightly greater than this) as well as double  $S_4$  events (mesonic x-rays followed by a nuclear capture count or afterpulsing), and various events inconsistent with the expected behavior of stopping muons. Category (f) is an indication of the number of protons accepted, while (g) is typical of the soft component. The last two types of events all showed zero delay, indicating that the spurious delayed events discussed in Sec. IIA have

<sup>10</sup> A restaurant "stock pot" made by the Vollrath Company, Sheboygan, Wisconsin.

<sup>11</sup> Hillas, Gilboy, and Tennent, *Phil. Mag.* **3**, 109 (1958).

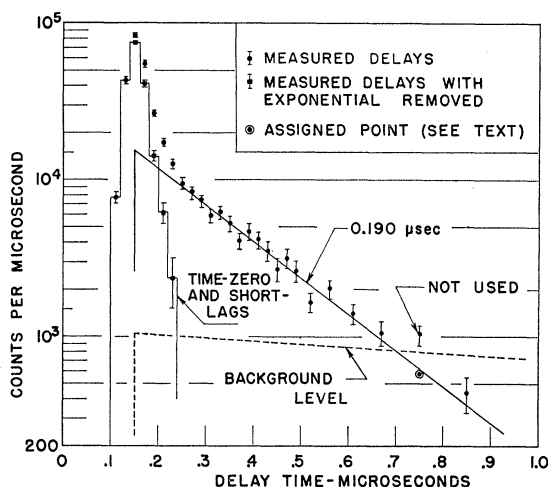


FIG. 3. Delay distribution for  $\mu^-$ -capture events. The final corrected value of the mean life was  $196 \pm 8$   $\mu\text{sec}$ , as stated in the text. The background removed is a composite of a 2.22- $\mu\text{sec}$  exponential distribution from  $\mu^+$  decays and a flat accidental distribution. The flags on each point are standard statistical deviations.

indeed been eliminated by the rigid muon selection system.

The accepted events were assigned to time delay channels with a width of 20  $\mu\text{sec}$  out of 1.5  $\mu\text{sec}$  and 0.5  $\mu\text{sec}$  thereafter. The delay distribution was analyzed into a flat background, a 2.2- $\mu\text{sec}$  exponential component, and a muon capture component. Figure 3 shows the delay distribution with the flat background and the 2.2- $\mu\text{sec}$  component removed. The zero on the time scale is at 150  $\mu\text{sec}$  to avoid bias in reading time zeros. The point at 0.75  $\mu\text{sec}$  (true delay 0.6  $\mu\text{sec}$ ) had to be corrected because of an ambiguity in film event selection for certain types of events with 0.6- $\mu\text{sec}$  delay. The correction was made using a run in which  $S_1$ ,  $S_2$ , and  $S_3$  were not artificially separated on the trace.

The slope of the delay distribution in Fig. 3 is shown as 0.190  $\mu\text{sec}$ . Our final best value was obtained by Peierl's method and includes an additional 3.5% correction for events where a delay in the target scintillators  $S_1$ ,  $S_2$ , or  $S_3$  could not be recognized (and rejected) because the delay was unresolved from a prompt pulse in the same scintillator. The correction was made by observing that the rejected delay events must have a 2.2- $\mu\text{sec}$  time distribution. Thus a deviation from the 2.2- $\mu\text{sec}$  exponential near the time origin of the events rejected by the target scintillators must be reflected in the accepted events distribution.

The  $\mu^-$  mean life in Fe, based on 1750 events, is found to be

$$\tau = 196 \pm 8 \mu\text{sec},$$

where a 6- $\mu\text{sec}$  error has been assigned to the corrections made and systematic errors, and the independent statistical standard error is also 6  $\mu\text{sec}$ .

That other systematic errors do not exist is substantiated in several ways:

(1) The decay curve follows a single exponential over 4 mean lives.

(2) A time delay distribution in the absence of a target showed no short-lag contamination.

(3) The capture mean life in Pb (which would be especially sensitive to short-component contamination) was found in a short run to be  $71 \pm 7$   $\mu\text{sec}$ , in good agreement with the results of Meyer and others.

(4) Periodic checks on instrumental errors revealed that an over-all precision of 1% was consistently maintained.

#### IV. DISCUSSION

Our result for the mean life in Fe is in excellent agreement with previous results, including those of Telegdi's group<sup>2</sup> ( $202 \pm 6$   $\mu\text{sec}$ ), and of Hillas, Gilboy, and Tennent<sup>11</sup> ( $201 \pm 11$   $\mu\text{sec}$ ). Combining these values with our own, we find for the best value of the disappearance rate (reciprocal of the mean life) the value

$$\lambda = (5.00 \pm 0.01) \times 10^6 \text{ sec}^{-1}.$$

A value of the rate  $\lambda_d$  for the spontaneous decay process  $\mu^- \rightarrow e + \nu + \bar{\nu}$  for muons bound in the mesonic K-orbit of Fe may now be obtained. Lederman and Weinrich<sup>1</sup> found that the fraction of muons disappearing by  $\mu-e$  decay was  $f_d = 0.103 \pm 0.005$ . Combining this with the best value for the total disappearance rate  $\lambda$ , we obtain

$$\lambda_d/\lambda_0 = 1.15 \pm 0.06,$$

where  $\lambda_0$  is the decay rate of the free muon,  $(0.451 \pm 0.004) \times 10^6 \text{ sec}^{-1}$ . This ratio is to be compared with the value  $1.21 \pm 0.05$  obtained by the Chicago group.<sup>3</sup> As stated in the introduction, theoretical interpretation of this result is still lacking. Existing theoretical treatments<sup>4,6</sup> would give a ratio around 0.8 to 0.9.

Further measurements of  $\lambda_d$  which include electron counting as well as the measurement of the delay distribution are now under way in this laboratory.

Small deviations from unity in the ratio  $\lambda_d/\lambda_0$ , such as we observe here, have a negligible effect of course on the capture rate  $\lambda_c = \lambda - \lambda_d$ . This is because, in medium and heavy elements,  $\lambda_d$  is small compared to  $\lambda$ . As shown by Sens *et al.*,<sup>2</sup> experiment and theory<sup>12</sup> with regard to  $\lambda_c$  are in good accord—a conclusion which is reinforced in a small way by the present paper.

<sup>12</sup> H. Primakoff, *Proceedings of the Fifth Annual Rochester Conference on High-Energy Physics* (Interscience Publishers, Inc., New York, 1955), p. 174.